

Article

A Novel MPPT Based Reptile Search Algorithm for Photovoltaic System under Various Conditions

Nadia Douifi ^{1,*}, Amel Abbadi ², Fethia Hamidia ², Khalid Yahya ³, Mahmoud Mohamed ^{4,*}
and Nawal Rai ¹

¹ Advanced Electronic Systems Laboratory (AESL), Electrical Engineering Department, Faculty of Technology, Dr. Yahia Fares University, Medea 26000, Algeria; rainawel27@gmail.com

² Electrical Engineering and Automatic Laboratory (EEAL), Electrical Engineering Department, Faculty of Technology, Dr. Yahia Fares University, Medea 26000, Algeria; amel.abbadi@yahoo.fr (A.A.); fe_hamidia@yahoo.fr (F.H.)

³ Department of Electrical and Electronics Engineering, Nisantasi University, Istanbul 34467, Turkey; khalid.yahya@nisantasi.edu.tr

⁴ School of Engineering, Cardiff University, Cardiff CF24 3AA, UK

* Correspondence: douifi.nadia@gmail.com (N.D.); mohamedmt@cardiff.ac.uk (M.M.)

Abstract: Solar systems connected to the grid are crucial in addressing the global energy crisis and meeting rising energy demand. The efficiency of these systems is totally impacted by varying weather conditions such as changes in irradiance and temperature throughout the day. Additionally, partial shading (PS) adds to the complexity of the nonlinear characteristics of photovoltaic (PV) systems, leading to significant power loss. To address this issue, maximum power point tracking (MPPT) algorithms have become an essential component in PV systems to ensure optimal power extraction. This paper introduces a new MPPT control technique based on a novel reptile search optimization algorithm (RSA). The effectiveness of the proposed RSA method is evaluated under different weather conditions with varying irradiance and partial shading. The results of the RSA algorithm are compared to other existing bio-inspired algorithms and show superior performance with an average efficiency of 99.91%, faster dynamic response of 50 ms, and less than 20 watts of oscillation. The RSA-MPPT based technique provides higher efficiency, faster settling time, and minimal oscillation around the maximum power point (MPP), making it a reliable solution for effective solar power harvesting.

Keywords: maximum power point; partial shading; photovoltaic system; power harvesting; reptile search optimization algorithm



Citation: Douifi, N.; Abbadi, A.; Hamidia, F.; Yahya, K.; Mohamed, M.; Rai, N. A Novel MPPT Based Reptile Search Algorithm for Photovoltaic System under Various Conditions. *Appl. Sci.* **2023**, *13*, 4866. <https://doi.org/10.3390/app13084866>

Academic Editor: Alejandro Pérez-Rodríguez

Received: 10 March 2023

Revised: 29 March 2023

Accepted: 11 April 2023

Published: 12 April 2023



Copyright: © 2023 by the authors. Licensee MDPI, Basel, Switzerland. This article is an open access article distributed under the terms and conditions of the Creative Commons Attribution (CC BY) license (<https://creativecommons.org/licenses/by/4.0/>).

1. Introduction

The world is currently facing a critical challenge in the form of global warming, which poses a threat to the global economy, the planet, and human survival. The primary cause of global warming is the increase in greenhouse gases in the atmosphere, largely due to human activities such as the burning of fossil fuels, industrialization, and urbanization. To address this issue, governments have started investing in renewable energy and developing new green technologies.

Solar energy is the most attractive of all renewable energy sources, providing electricity to the world [1]. Solar photovoltaic systems are particularly popular due to their simplicity of installation, availability of sunlight, low maintenance cost, and silent operation. These systems generate electricity through the photoelectric effect using the sun's energy [2]. Despite numerous efforts to improve the operational performance of PV systems, the nonlinear characteristics and low power conversion efficiency remain major challenges and limitations in their integration into power grids. Furthermore, the generation of PV power is heavily dependent on atmospheric conditions (temperature and radiation), which

are constantly changing throughout the day [3–5]. This challenge is further compounded in the case of partial shading, which occurs when solar radiation is unevenly distributed across the PV system's array due to obstacles such as clouds, trees, and buildings in the surrounding area [6]. To address these challenges and issues, PV systems are equipped with a special controller, known as MPPT controller.

The role of the MPPT controller in the PV system is crucial to optimizing the generated electricity and increasing the overall efficiency. The controller, which is guided by a sophisticated control algorithm, regulates the DC-DC converter duty cycle to make sure the global maximum power point (GMPP) is consistently tracked under varying operational conditions [7,8].

Several traditional MPPT tracking methods, including Perturb and Observe (P&O) [9], Incremental Conductance (INC) [10], and Hill Climbing (HC) [11], have been introduced over the years. These algorithms are simple and easy to implement, but they can suffer from steady-state oscillation, slow convergence, and potential for maximum power tracking failure when subjected to rapidly changing irradiance or partial shading conditions. Many works such as [12–15] have been carried out to overcome these drawbacks by utilizing a variable step size rather than a fixed step size. A certain improvement in power efficiency and tracking speed has been noticed but the oscillation problem that leads to power losses was not well avoided and the complexity of the newly introduced algorithm had increased compared to the conventional methods.

To address these shortcomings of conventional methods, various bio-inspired meta-heuristic algorithms have been proposed in the literature. In [16] new Particle Swarm Optimization (PSO) algorithm based on Lagrange Interpolation is proposed. This strategy solved the difficulties of the traditional method by employing a numerical computation to initialize the particles around the Global point. Although the proposed algorithm showed good accuracy in reaching MPP and superior stability around this point in steady radiation scenarios, its convergence rate is low in varying radiation conditions, and it is hard to implement in practical mode.

In [17,18], Grey Wolf Optimization (GWO) and Artificial Bee Colony (ABC) algorithms were proposed; both algorithms showed a good performance in MPP tracking but with drawbacks of high complexity, computational time, and cost. Further drawbacks of these algorithms include difficulties with parameter initialization and calculation in a large population. To solve the MPPT problem, the author of [19] provided an Ant Colony Optimization (ACO) method with a novel pheromone update; the introduced algorithm showed good robustness, high efficiency, and fast convergence speed in tracking the true MPP of the system. However, practical implementation, the complexity of computation, and high cost are the main constraints to the adaptation of these approaches in real-time scenarios.

Reference [20] presented a new MPPT based on Dragonfly Optimization (DOA) algorithm; results indicated that the suggested DOA approach outperforms previous strategies in terms of power efficiency and response time. The main drawback of this algorithm is transient oscillation. In [21], a marine predator algorithm-based MPPT control technique is introduced. This algorithm mimics the predator-prey relationship found in marine species. The experimental findings demonstrate that this approach can accomplish good tracking abilities under various external situations. However, its convergence speed was low, and its performance was affected by the initial conditions. Refs. [22,23] proposed Fish Swarm Optimization (FSO) and Whale Optimization Algorithm (WOA) algorithms, respectively. Abilities of these algorithms to approach the global maximum under partially shaded situations are significantly impacted, and its implementation is becoming more challenging because the training required is quite extensive. Reference [24] introduced a hybrid shuffled frog-leaping and pattern search algorithm (HSFLA-PS) for MPPT; the hybrid approach was able to identify the global maximum power peak in distinct climatic scenarios with a high convergence rate and efficiency, according to the presented results. Though, the complexity of the proposed HSFLA-PS MPPT controller can make it more difficult to design, and implement in a real-world PV system.

In [25], the author suggested an additional filtration and distribution procedure called Random walk in addition to the ordering of solutions to develop a new algorithm called Ordered Flower Pollination Algorithm. The proposed algorithm (Ordered FPA) has outperformed the well-known FPA algorithm [26] under different weather circumstances. Ref. [27] suggests a novel MPPT controller for a hybrid system. It employs IFFO-FLC to tune the controller parameters. Results showed that the proposed algorithm provided better performance in terms of convergence speed and high efficiency compared to the other algorithms. However, it requires multiple parameters tuning, which can be a time-consuming and challenging task.

After a critical evaluation of all the published algorithms, it observed that, although many of them have shown effectiveness in global MPPT searches, sometimes they show disappointing performance in some circumstances by getting stuck at local maximum power point. In other words, the published algorithms' best performance is not always guaranteed, and it depends on the complexity of the PV system and operational conditions. From this perspective, developing or applying a new intelligent algorithm with higher potential for MPPT application has always been encouraged to improve MPP search performance.

Following a thorough literature research on the newly introduced intelligent optimization algorithms, Reptile Search Optimization (RSA) algorithm has been noted due to its efficacy, strength, adaptive capabilities, and notable design. RSA has a unique method of updating solution positions through four mechanisms. This unique mechanism allows the algorithm to preserve diversity among potential solutions while identifying the optimal one. Moreover, it ensures continuity of exploration, especially in the case of local optima stagnation in the last iterations. This algorithm can efficiently track the global solution and avoids local optima.

Taking into account the abovementioned facts, the authors are motivated to apply the RSA algorithm to extract the maximum power of a grid-connected PV system under different weather scenarios. The main contribution of this study is to develop a large-scale PV system with an effective MPPT controller based on the new RSA algorithm to track GMPP under various climatic circumstances. The efficiency and performance of the proposed RSA algorithm were tested under varying solar irradiance and partial shading conditions, and then compared with different bio-inspired optimization MPPT methods. The suggested RSA-MPPT based method is found to have remarkable performance in terms of tracking efficiency, faster convergence time, and robustness (under fast and slow variation of irradiance), higher tracking accuracy, and better global tracking capabilities.

The rest of the paper is organized as follows: the PV system description and the impact of variable irradiance and partial shading on PV characteristics are discussed in Section 2, proposed RSA-MPPT algorithm is presented in Section 3, simulation results are presented and analyzed in Section 4, and finally, conclusion remarks are given in Section 5.

2. PV System Configuration

The PV system topology in this study is depicted in Figure 1. It is a large-scale, three-phase, grid-connected system composed of a PV array, a DC-DC boost converter with an MPPT controller, and a three-phase VSC inverter. The PV array consists of 60 parallel strings, each composed of 5 modules connected in series, and it is rearranged into three PV arrays connected in series. The system is designed to generate a maximum output of 100.37 KW under Standard Test Conditions (STC) (irradiance 1000 KW/m² and temperature 25 °C).

Impact of Irradiance and Shading on the PV System

Figure 2a illustrates the effect of uniform solar radiation on the P-V curves of the PV array. As the irradiance increases, the generated power also increases and vice versa [28]. There exists a single point, referred to as the MPP, where the power generated is at its maximum, and to operate the PV array at this point, the impedance of the PV and the load must be matched with the use of an MPPT tracker [29].

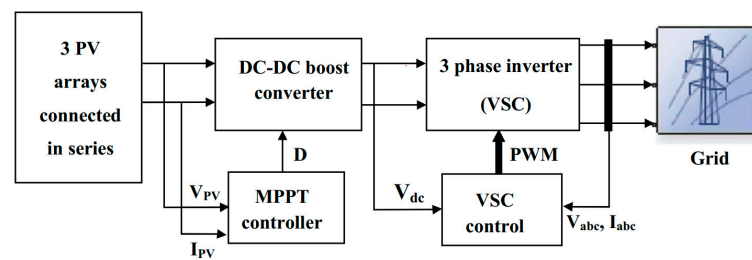


Figure 1. Block diagram of the grid connected PV system.

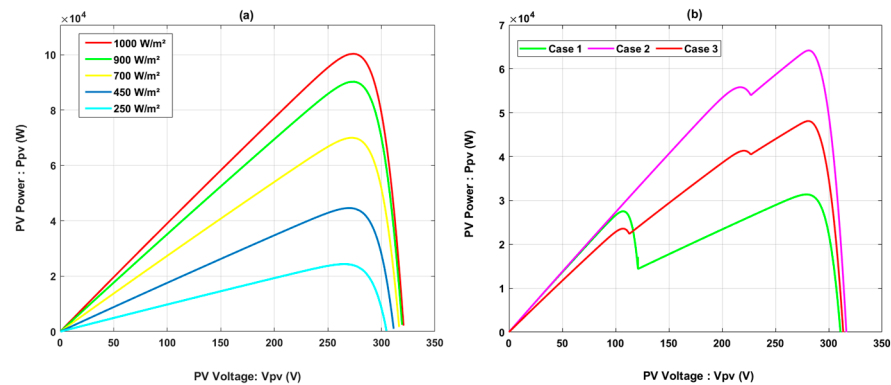


Figure 2. PV characteristic curves (a) under uniform solar irradiance and (b) under PSC.

Another issue that affects the efficiency of the PV system, besides variations in weather conditions, is partial shading. This phenomenon has a great and serious influence on the characteristics of the PV module; it occurs when some of the PV modules connected in a string receive a different level of insolation [30,31]. To prevent hotspot problems and current mismatches caused by partial shading, bypass diodes are placed in parallel with each PV module. Additionally, a blocking diode is connected to prevent current flow from the unshaded modules to the shaded modules [32].

While the bypass diode allows the PV system to operate efficiently under partial shading conditions, it also makes the curves of the PV array complex, resulting in multiple peaks with only one global peak known as the GMPP (Figure 2b), making it challenging to track the maximum power. After examining the nonlinear characteristics of the PV array and the effects of various factors on its efficiency, an MPPT tracker with appropriate optimization techniques is deemed critical to enhancing the performance of the system. It extracts the available maximum power by operating the PV array at the GMPP.

3. Reptile Search Optimization (RSA) Based MPPT Algorithm

RSA is a new biomimetic meta-heuristic optimization algorithm that was originally introduced by [33]. It is a swarm-based and gradient-free method that can solve and treat difficult problems exposed to specific constraints. RSA is derived from encircling, hunting and natural social behavior of crocodiles, and it has its own strategy for updating position of candidates. RSA basically varied between exploration (Encircling) and exploitation (Hunting) phases that describe the global and local search mechanisms based on the number of iterations [33].

3.1. RSA Algorithm for MPPT

The proposed modifications to the traditional RSA algorithm make it suitable for use in MPPT of PV systems. The algorithm continuously reads the output voltage and current of the PV array, as depicted in the flowchart of the algorithm in Figure 3. This information is then utilized to calculate the output power, which serves as a validity function that helps to update and determine the next duty cycle of the boost converter until the optimum duty cycle (D_{Best}) is reached. The RSA algorithm employs two main techniques, encircling and

hunting, to update the position of the candidate duty cycle (D). The following sub-sections will elaborate on these techniques and provide a detailed mathematical model.

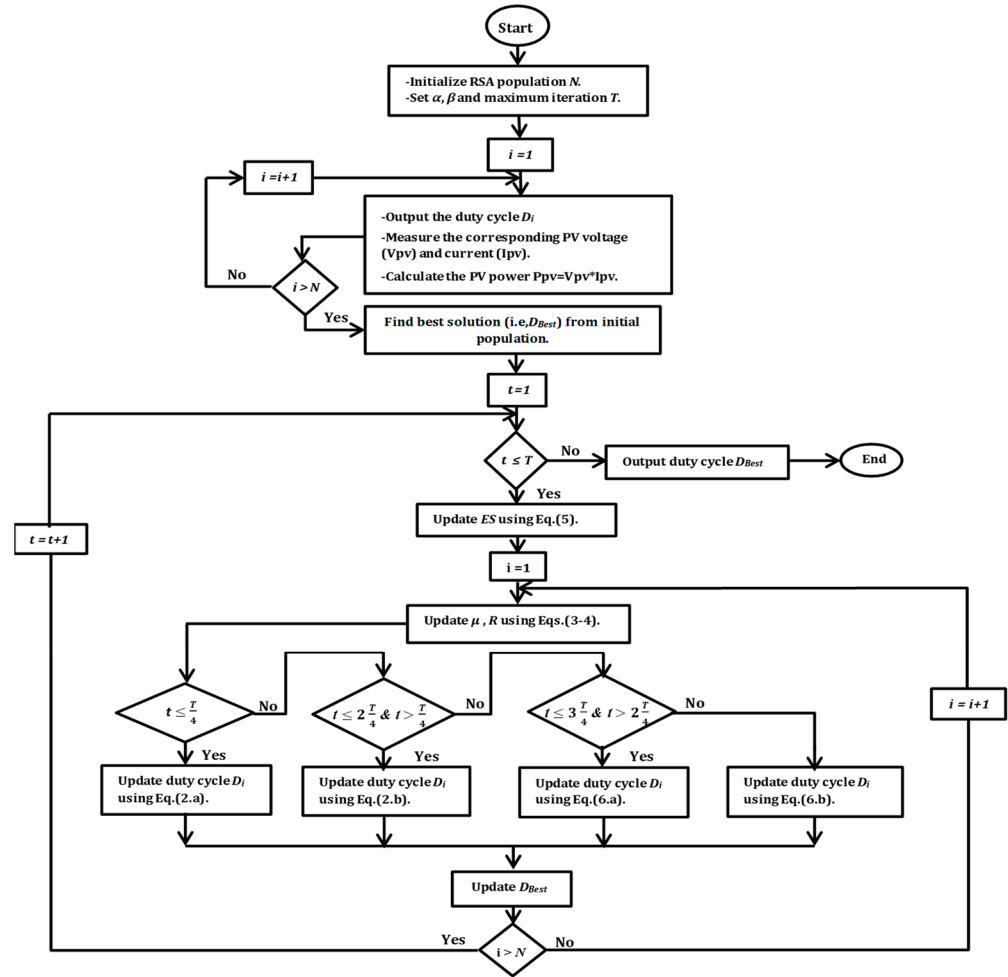


Figure 3. RSA-MPPT based flowchart.

3.1.1. Initialization

The initial phase of the RSA-MPPT based algorithm involves the selection of a random set of candidate solutions in the form of duty cycles.

$$D_i = rand(D_{max} - D_{min}) + D_{min} \tag{1}$$

D_{max} and D_{min} are maximum and minimum values of the duty ratio.

The RSA algorithm operates in two phases: firstly, it performs the encircling mechanism for the first half of the total number of iterations and then switches to the exploitation (hunting) mechanism for the second half.

3.1.2. Encircling Phase (Exploration)

According to the behavior of crocodiles during the encircling phase, they use two different strategies to move in the search space: (high walking and belly walking). These two walking techniques are performed in this level of optimization to support the hunting phase in the search area and produce more distinct solutions and investigate several regions. During this phase of the search, the high walking transportation strategy is performed only when $t \leq \frac{T}{4}$ and belly walking strategy is performed only if $t > \frac{T}{4}$ and $t \leq \frac{2T}{4}$ where t is

the current iteration [33]. Then duty cycle in the exploration phase is updated according to Equation (2).

$$D_i(t+1) = \begin{cases} D_{Best}(t) - \eta_i(t) \times \beta - R_i(t) \times rand & t \leq \frac{T}{4} \quad (a) \\ D_{Best}(t) \times D_{r_1} \times ES(t) \times rand & t \leq 2\frac{T}{4} \text{ and } t > \frac{T}{4} \quad (b) \end{cases} \quad (2)$$

where $\eta_i(t)$ is the hunting parameter; it is beneficial to ensure exploration continuity and avoid getting stuck in local optima, especially in the last iterations. It is calculated using Equation (3). R_i denotes Reduce function, which is used to reduce search area, and it is calculated using Equation (4). Evolutionary ratio $ES(t)$ is a probability ratio that decreases arbitrarily between $[2, -2]$ over the number of iterations to maintain diversity among potential solutions. It is calculated using Equation (5).

$$\eta_i = D_{Best}(t) \times \alpha \quad (3)$$

$$R_i = \frac{D_{Best}(t) - D_{r_2}}{D_{Best}(t) + \varepsilon} \quad (4)$$

$$ES(t) = 2 \times r_3 \times \left(1 - \frac{t}{T}\right) \quad (5)$$

D_{Best} is the best duty cycle obtained so far, T is maximum number of iterations, $rand$ is random value between 0 and 1, r_1 and r_2 are random numbers between $[1, N]$ where N is population size. D_{r_1} , D_{r_2} are random duty cycle positions. β is a sensitive parameter that regulates the encircling phase’s exploration accuracy (high walking) during iterations; in this paper, it is fixed at value 0.005. r_3 is random integer number between -1 and 1 . α is also a critical parameter that determines the exploration accuracy for hunting partnership. It is fixed at value 0.1 in this paper.

3.1.3. Hunting Phase

The exploiting behavior shows that crocodiles use two strategies to hunt their prey (hunting coordination and hunting cooperation). These techniques are performed at this stage of optimization to conduct the local search and ensure reaching the optimal solution. The hunting techniques are executed according to following conditions; where: hunting coordination technique is performed when $t > \frac{2T}{4}$ and $t \leq \frac{3T}{4}$ and hunting cooperation is executed when $t > \frac{3T}{4}$ and $t \leq T$ [22]. The duty cycle then; is updated based on the following equation:

$$D_i(t+1) = \begin{cases} D_{Best}(t) \times \alpha \times rand & t \leq 3\frac{T}{4} \text{ and } t > 2\frac{T}{4} \quad (a) \\ D_{Best}(t) - \eta_i(t) \times \varepsilon - R_i(t) \times rand & t \leq T \text{ and } t > 3\frac{T}{4} \quad (b) \end{cases} \quad (6)$$

The evaluation of computational complexity is crucial in determining an algorithm’s efficiency, as it influences the execution time and memory resources required for implementation. In this context, the proposed RSA-based MPPT algorithm’s computational complexity has been analyzed in detail by [33]. The time complexity of the RSA algorithm is expressed as $O(T \times N) + O(T \times N \times D)$. Where T is the number of iterations, N is the population size, and D is the solution size. This linear growth with the increase in input size makes it suitable for real-time applications. Compared to other MPPT techniques, such as DOA, WOA, GWO, and PSO, the RSA algorithm exhibits lower time complexity, resulting in faster execution times and quicker convergence to the optimal solution. It is important to note that the efficiency of the RSA algorithm might be affected by parameter choices, such as population size, number of iterations, and sensitive parameters (β and α); thus, further optimization may be necessary for optimal performance in various applications.

4. Results and Discussion

In this section, the MPPT PV system depicted in Figure 1 is modelled and simulated using the MATLAB/SIMULINK software. The efficacy of the recommended RSA-MPPT controller is evaluated, and its performance is demonstrated through two simulation analyses, which are compared against DOA [20], WOA [23], GWO [17], and PSO [16] algorithms. Table 1 presents the settings of parameters, iteration number T , and population size N of each simulated algorithm.

Table 1. Setting of optimization algorithms' parameters.

| | Parameters | Iteration Number T | Population Size N |
|-----|---|----------------------|---------------------|
| RSA | $\beta = 0.005, \alpha = 0.1$ | 4 | 5 |
| DOA | ω, a, b, c, d and e are calculated in the program. | 9 | 6 |
| GWO | α, β, γ are calculated in the program. | 15 | 10 |
| WOA | $m = 1.5, R_c = \text{rand}, l$ is calculated in the program. | 5 | 7 |
| PSO | $c_1 = c_2 = 1.5, \omega = [0.4, 0.99]$ | 10 | 5 |

The first simulation is conducted under uniform solar irradiance (USI) conditions, which entail slow and gradual changes in irradiance as well as rapid fluctuations. In the second simulation, the performance of the RSA-based MPPT controller is examined in various partial shading scenarios (PSCs).

During all the simulations, the control of the boost and VSC is initially blocked for 0.05 s for the purpose of regulating the system. Following this, the blocking is removed, and the duty cycle of the boost converter is set to a fixed value of $D = 0.5$. This configuration persists until the MPPT is enabled at $t = 0.4$ s. The impact of this procedure is evident in the resulting waveforms.

4.1. Uniform Solar Irradiance Condition (USI)

Under uniform solar illumination, the level of radiation received by PV arrays is consistent, but it undergoes gradual and rapid variations over time. The irradiance profile utilized in this simulation to test the Proposed RSA algorithm under USI conditions is presented in Figure 4. The ambient temperature is maintained at a fixed value of $T = 25$ °C. As shown in the figure, irradiance changes successively and rapidly between different high and low levels, with both small and wide variations. For instance, there is a gradual decrease in irradiance from 1000 to 250 KW/m².

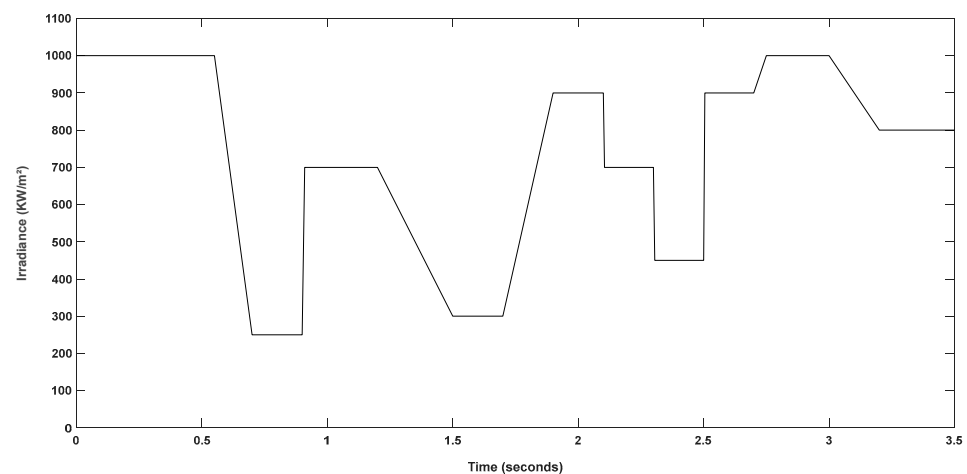


Figure 4. Illumination profile of the uniform solar irradiance condition (USI).

The comparison of simulation results is depicted in Figure 5, with certain portions of the resulting power curves being magnified in Figure 6 to enable a more thorough evaluation of the performance of the proposed RSA-MPPT algorithm. A comprehensive analysis of the algorithm’s performance is presented in Table 2, including the power extracted at the MPP, settling time, power efficiency, and steady-state oscillation.

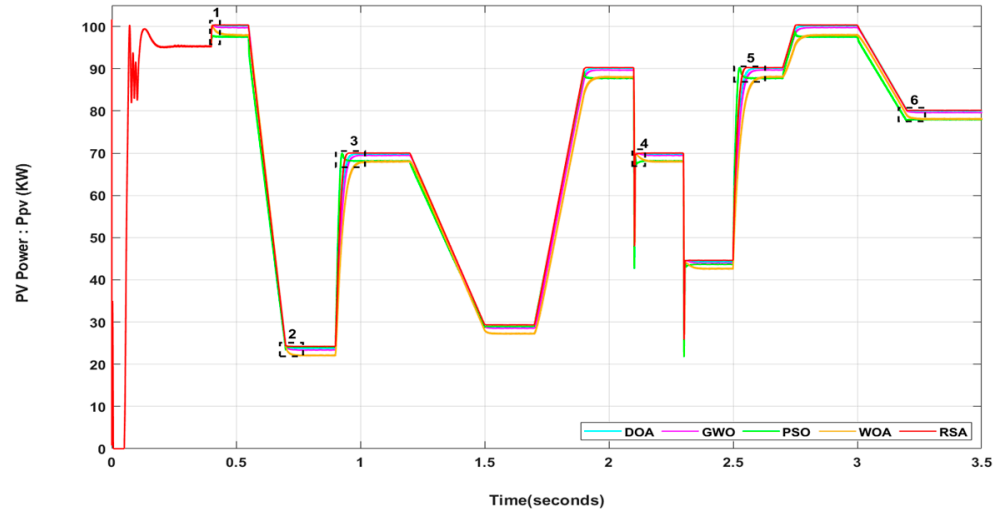


Figure 5. PV output power (P_{pv}) under USI condition.

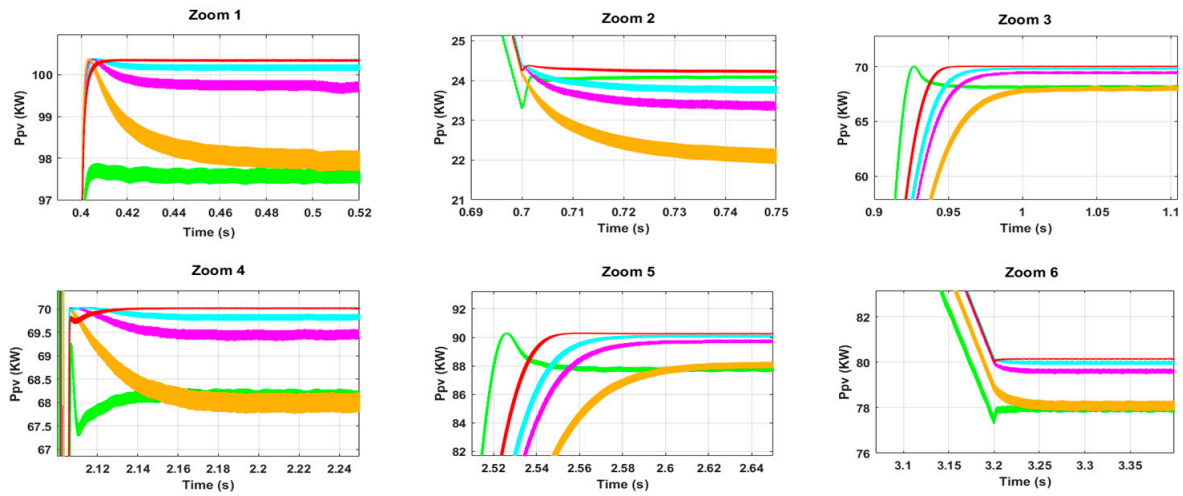


Figure 6. Zoomed parts of the PV output power waveform.

At $t = 0.55$ s, a wide variation occurred when the irradiance gradually decreased from 1000 to 250 KW/m^2 . The RSA algorithm achieved the highest efficiency of 99.47% , followed by PSO, DOA, GWO, and WOA, with efficiencies of: 98.79% , 97.68% , 95.92% , and 90.87% , respectively. The RSA-MPPT tracker settled at the MPP in the shortest time, taking only 25 ms, compared to DOA, WOA, GWO, and PSO, which took 40 ms, 60 ms, 50 ms, and 50 ms, respectively. The results demonstrate that, in both cases of rapid increase and decrease in PV irradiance, the power extracted by the RSA algorithm was the closest to the theoretical values, with good tracking rapidity and the highest efficiency of around 99.98% . The other tested algorithms were slower in finding the optimal MPP, and their efficiencies ranged from 90.87% to 99.83% .

Table 2. Comparison of USI simulation results.

| | | | | | | | | | | | |
|-----|--------------------------|------------|---------|----------|---------|---------|-----------|-----------|-----------|--------|--------|
| | | 0.4–0.55 | 0.7–0.9 | 0.91–1.2 | 1.5–1.7 | 1.9–2.1 | 2.105–2.3 | 2.305–2.5 | 2.505–2.7 | 2.75–3 | 3.2–4 |
| RSA | P _{actual} (KW) | 100.37 | 24.374 | 70.028 | 29.42 | 90.28 | 70.028 | 44.625 | 90.28 | 100.37 | 80.171 |
| | P _{mpp} (KW) | 100.34 | 24.245 | 70.02 | 29.34 | 90.26 | 70.02 | 44.616 | 90.26 | 100.34 | 80.16 |
| | Tr (s) | 0.415 | 0.725 | 0.96 | 1.52 | 1.925 | 2.14 | 2.16 | 2.56 | 2.765 | 3.21 |
| | η (%) | 99.97% | 99.47% | 99.99% | 99.72% | 99.98% | 99.99% | 99.98% | 99.98% | 99.97% | 99.98% |
| | Oscillation | ≈20 Watts | | | | | | | | | |
| DOA | P _{mpp} (KW) | 100.2 | 23.81 | 69.84 | 28.93 | 90.12 | 69.84 | 44.33 | 90.12 | 100.18 | 79.98 |
| | Tr (s) | 0.428 | 0.74 | 1.01 | 1.59 | 1.98 | 2.22 | 2.41 | 2.595 | 2.82 | 3.25 |
| | η (%) | 99.83% | 97.68% | 99.73% | 98.33% | 99.82% | 99.73% | 99.33% | 99.82% | 99.81% | 99.76% |
| | Oscillation | ≈60 Watts | | | | | | | | | |
| WOA | P _{mpp} (KW) | 98 | 22.15 | 68 | 27.25 | 88.2 | 68 | 42.75 | 88.2 | 98 | 78.2 |
| | Tr (s) | 0.5 | 0.76 | 1.05 | 1.55 | 2 | 2.19 | 2.43 | 2.65 | 2.85 | 3.27 |
| | η (%) | 97.64% | 90.87% | 97.10% | 92.62% | 97.69% | 97.10% | 95.80% | 97.69% | 97.64% | 97.54% |
| | Oscillation | ≈280 Watts | | | | | | | | | |
| GWO | P _{mpp} (KW) | 99.7 | 23.38 | 69.5 | 28.55 | 89.68 | 69.45 | 43.95 | 89.75 | 99.75 | 79.68 |
| | Tr (s) | 0.5 | 0.75 | 1.12 | 1.53 | 2.02 | 2.16 | 2.38 | 2.62 | 2.83 | 3.25 |
| | η (%) | 99.33% | 95.92% | 99.24% | 97.04% | 99.33% | 99.17% | 98.49% | 99.41% | 99.38% | 99.39% |
| | Oscillation | ≈100 Watts | | | | | | | | | |
| PSO | P _{mpp} (KW) | 97.58 | 24.08 | 68.15 | 28.97 | 87.80 | 68.17 | 43.65 | 87.78 | 97.62 | 77.96 |
| | Tr (s) | 0.44 | 0.75 | 0.975 | 1.53 | 1.95 | 2.155 | 2.57 | 2.73 | 2.975 | 3.23 |
| | η (%) | 97.22% | 98.79% | 97.32% | 98.47% | 97.25% | 97.34% | 97.82% | 97.23 | 97.26% | 97.24% |
| | Oscillation | ≈80 Watts | | | | | | | | | |

Additionally, as indicated in Figure 6, the developed RSA-MPPT algorithm exhibited the least fluctuation and steady-state power oscillation around the MPP point, with fluctuations below 20 watts. This indicates that in cases of variable irradiance, the new RSA method has the capability to reduce steady-state oscillation by 66.67% compared to DOA, 92.85% compared to WOA, 80% compared to GWO, and 75% compared to PSO.

4.2. Non Uniform Irradiance Condition

The MPP tracking under non-uniform irradiance conditions, specifically partial shading, is known to be a challenging task due to the presence of multiple peaks in the I-V/P-V characteristic curves. The number of peaks depends on the number of shaded modules in the PV array. To comprehensively evaluate the global peak tracking capabilities of the proposed RSA algorithm, three different shading patterns were applied to the three PV arrays connected in series. The irradiance arrangements of these shading patterns are presented in Table 3, while their corresponding characteristic curves are displayed in Figure 2b. The simulation results of actual power accumulated by the PV system under PSC for case 1, case 2, and case 3 are shown in Figures 7–9, respectively. These results were obtained using the RSA, DOA, GWO, WOA, and PSO algorithms.

Table 3. Partial shading cases.

| Partial Shading ($T = 25\text{ }^{\circ}\text{C}$) | PV1 (w/m^2) | PV2 (w/m^2) | PV3 (w/m^2) | GMPP (K Watts) |
|--|------------------------|------------------------|------------------------|----------------|
| PSC Case1 | 700 | 300 | 300 | 31.37 KW |
| PSC Case2 | 700 | 700 | 600 | 64.19 KW |
| PSC Case 3 | 500 | 600 | 450 | 48.10 KW |

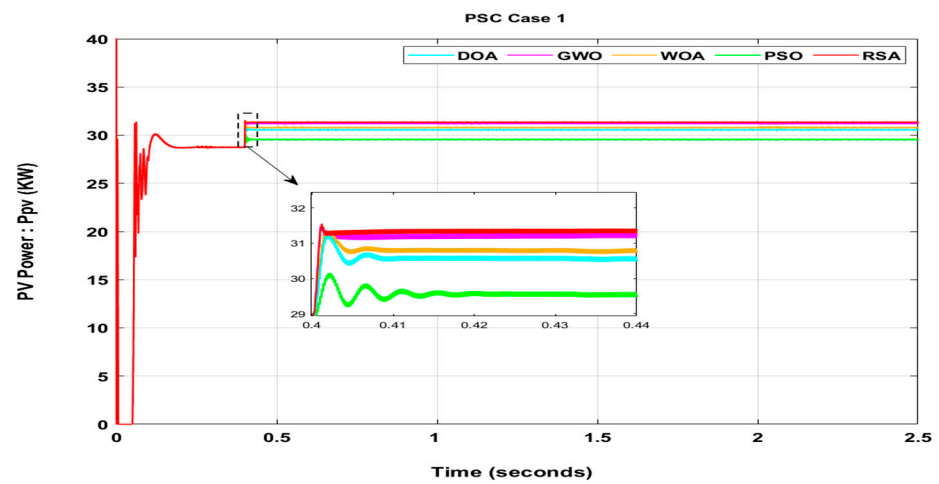


Figure 7. PV output power under PSC case 1.

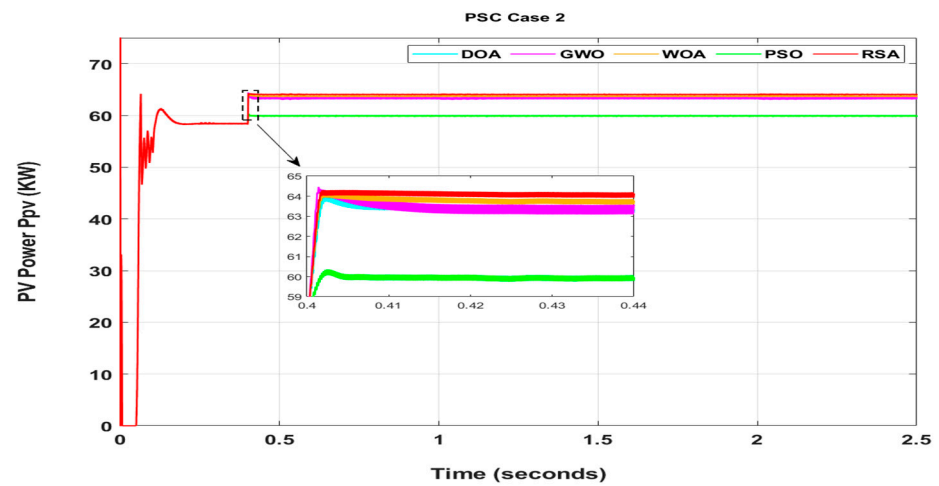


Figure 8. PV output power under PSC case 2.

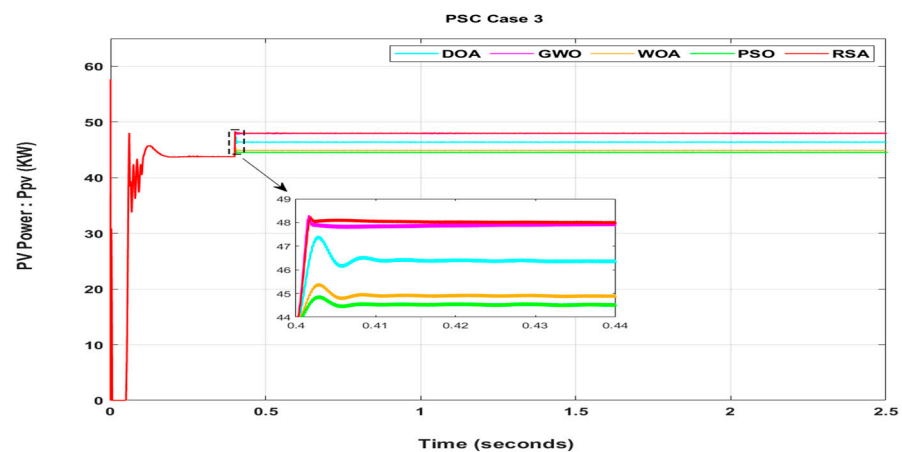


Figure 9. PV output power under PSC case 3.

Table 4 presents a summary of the exact values for extracted power (P_{mpp}), settling time (T_s) required to reach the MPP, and tracking efficiency (η) for each of the simulated MPPT algorithms under PSC.

Table 4. Comparison of PSC simulation results.

| | | PSC Case 1 | PSC Case 2 | PSC Case 3 |
|-----|----------------|------------|------------|------------|
| RSA | P_{mpp} (KW) | 31.35 KW | 64.15 | 48.03 |
| | T_s (s) | 0.41 | 0.416 | 0.425 |
| | η (%) | 99.94% | 99.94% | 99.85% |
| DOA | P_{mpp} (KW) | 30.57 | 63.30 | 46.38 |
| | T_s (s) | 0.43 | 0.435 | 0.43 |
| | η (%) | 97.45% | 98.61% | 96.43% |
| GWO | P_{mpp} (KW) | 31.28 | 63.59 | 47.92 |
| | T_s (s) | 0.435 | 0.42 | 0.44 |
| | η (%) | 99.71% | 99.07% | 99.63% |
| WOA | P_{mpp} (KW) | 30.79 | 63.75 | 44.91 |
| | T_s (s) | 0.42 | 0.425 | 0.432 |
| | η (%) | 98.15% | 99.32% | 93.37% |
| PSO | P_{mpp} (KW) | 29.56 | 59.92 | 44.55 |
| | T_s (s) | 0.426 | 0.42 | 0.438 |
| | η (%) | 94.23% | 93.35% | 92.62% |

Case 1: The first PV array (PV1) in this case is subjected to a different irradiance level compared to the other two arrays, resulting in a power voltage curve with two peaks and only one global peak at a power level of 31.37 KW, as shown in Figure 2b. The simulation results in Figure 7 demonstrate that the RSA-MPPT based algorithm achieved the global maximum power point (GMPP) with the highest efficiency of 99.94% among all the tested algorithms, followed by GWO with 99.71% and WOA with 98.15%. DOA obtained an efficiency of 97.45%, while the PSO algorithm had the least efficiency of about 94.23%. Furthermore, the RSA algorithm was the fastest in settling at the global peak in less than 10 ms, while the other algorithms took more time due to the fluctuations they exhibited.

Case 2: only one of the PV arrays (PV3) is partially shaded while the other two arrays receive the same level of irradiance. However, the difference in irradiance level between the arrays is small compared to Case 1. The PV curve (Figure 2b) exhibits the same behavior as Case 1, with a global maximum power of 64.19 KW.

Based on the simulation results presented in Figure 8, the RSA-MPPT algorithm outperformed the other algorithms. It achieved a convergence to the GMPP of 64.15 KW with 99.94% efficiency in just 16 ms. The WOA algorithm maintained a high efficiency rate of 99.32% in 25 ms, while the GWO method achieved a 99.07% efficiency rate in 20 ms. The DOA technique sustained an efficacy of about 98.61% in 35 ms, whereas the PSO algorithm attained a 93.35% efficiency in 20 ms. As seen in Figure 8, DOA, WOA, and PSO algorithms exhibited less fluctuation compared to the previous case of PSC.

Case 3: In this PSC scenario, the three series-connected PV arrays are subject to different degrees of shading. The resulting P-V curve, as shown in Figure 2, exhibits a single global peak and two local peaks at power levels of 48.10 KW, 41.34 KW, and 23.58 KW, respectively.

The overall results demonstrate that the proposed RSA algorithm exhibited superior performance and higher efficiency compared to the other examined methods. Figure 9 shows that RSA, GWO, DOA, WOA, and PSO techniques extracted output powers of 48.03 KW, 47.92 KW, 46.38 KW, 44.91 KW, and 44.55 KW, respectively. The RSA technique was not affected by the local peaks and achieved GMPP within 25 ms with the highest efficiency of approximately 99.85%. The GWO method maintained 99.63% efficiency in 40 ms. The DOA algorithm attained a 96.43% efficiency rate in 30 ms, while the WOA technique

upheld an efficacy of about 93.38% in 32 ms. The lowest efficiency of approximately 92.62% was obtained by the PSO algorithm in 38 ms.

The RSA-based MPPT algorithm demonstrates promising computational complexity properties, rendering it a reliable and efficient solution for solar power harvesting under various conditions. Therefore, there are many applications where the proposed RSA algorithm can be used, especially, for low voltage and power harvesting applications. One example of a similar application is the optimization of wind turbine performance. Since the proposed algorithm shows a good performance in tracking the global maximum power point of PV systems, the algorithm can be easily used to optimize the wind turbine performance by constantly adjusting the pitch and yaw of the turbine blades based on the measurement of wind's speed and direction. This algorithm can be also used in a solar tracking system to adjust the orientation of PV panels based on the sun's position. By training the algorithm on a dataset of panels' orientations and corresponding power outputs, it can quickly predict the optimal orientation of a PV panel for a given time and location.

5. Conclusions

In this article a new bio-inspired RSA based MPPT algorithm is introduced to maximize the power extracted from a grid connected PV system under various weather conditions. The RSA algorithm was first tested under uniform varying irradiance condition with gradual and rapid change. After that, Performance of the proposed technique was analyzed under three different scenarios of PSC. The obtained results were evaluated and compared with prominent MPPT techniques in regard to many criteria. The results examination and evaluation show that RSA algorithm outperformed the other simulated techniques in terms of power efficiency, settling time and oscillation in the transient state. Furthermore, in varying irradiance condition RSA method shows a high tracking efficiency with an average of 99.90% through the different irradiation levels, smallest steady state oscillation of less than 20 watts and shorter settling time. Moreover, an average efficiency of 99.91% was reported under PSC. However, the proposed RSA MPPT algorithm still has some limitations including steady state oscillations especially in case of partial shading conditions, and difficulties in parameters initialization. The remarkable results from the novel RSA-MPPT based technique prove its efficacy and superiority in enhancing the optimal power of the PV system, especially when the efficiency is the main criteria.

Author Contributions: Conceptualization, N.D.; Methodology, N.D.; software, N.D. and A.A.; validation, N.D. and K.Y.; formal analysis, N.D., K.Y. and N.R.; investigation, N.D., A.A., F.H., K.Y., M.M. and N.R.; Resources, K.Y. and M.M.; Data curation, N.D. and N.R.; writing—original draft preparation, N.D.; writing—review and editing, N.D., A.A., F.H., K.Y., M.M. and N.R.; visualization, F.H.; supervision, A.A. and F.H.; funding acquisition, M.M. All authors have read and agreed to the published version of the manuscript.

Funding: This research received no external funding.

Institutional Review Board Statement: Not applicable.

Informed Consent Statement: Not applicable.

Data Availability Statement: The data presented in this study are available upon request from the corresponding authors.

Conflicts of Interest: The authors declare no conflict of interest.

References

1. Ali, Z.M.; Alquthami, T.; Alkhalaf, S.; Norouzi, H.; Dadfar, S.; Suzuki, K. Novel hybrid improved bat algorithm and fuzzy system based MPPT for photovoltaic under variable atmospheric conditions. *Sustain. Energy Technol. Assess.* **2022**, *52*, 102156. [[CrossRef](#)]
2. Awan, M.M.A.; Javed, M.Y.; Asghar, A.B.; Ejsmont, K. Performance Optimization of a Ten Check MPPT Algorithm for an Off-Grid Solar Photovoltaic System. *Energies* **2022**, *15*, 2104. [[CrossRef](#)]

3. Rasheed, M.; Mohammed, O.Y.; Shihab, S.; Al-Adili, A. A comparative analysis of PV cell mathematical model. *J. Phys. Conf. Ser.* **2021**, *1795*, 012042. [[CrossRef](#)]
4. Giurgi, G.I.; Szolga, L.A.; Giurgi, D.V. Benefits of fuzzy logic on MPPT and PI controllers in the chain of photovoltaic control systems. *Appl. Sci.* **2022**, *12*, 2318. [[CrossRef](#)]
5. Deboucha, H.; Mekhilef, S.; Belaid, S.; Guichi, A. Modified deterministic Jaya (DM-Jaya)-based MPPT algorithm under partially shaded conditions for PV system. *IET Power Electron.* **2020**, *13*, 4625–4632. [[CrossRef](#)]
6. Chtita, S.; Motahhir, S.; El Hammoumi, A.; Chouder, A.; Benyoucef, A.S.; El Ghzizal, A.; Derouich, A.; Abouhawwash, M.; Askar, S.S. A novel hybrid GWO–PSO-based maximum power point tracking for photovoltaic systems operating under partial shading conditions. *Sci. Rep.* **2022**, *12*, 10637. [[CrossRef](#)] [[PubMed](#)]
7. Pradhan, C.; Senapati, M.K.; Ntiakoh, N.K.; Calay, R.K. Roach Infestation Optimization MPPT Algorithm for Solar Photovoltaic System. *Electronics* **2022**, *11*, 927. [[CrossRef](#)]
8. Doubabi, H.; Salhi, I.; Chennani, M.; Essounbouli, N. High Performance MPPT based on TS Fuzzy–integral backstepping control for PV system under rapid varying irradiance—Experimental validation. *ISA Trans.* **2021**, *118*, 247–259. [[CrossRef](#)]
9. Kumar, H.; Sharma, A.K. Performance analysis of maximum power point tracking algorithms for grid connected PV system. In Proceedings of the 2014 6th IEEE Power India International Conference (PIICON), Delhi, India, 5–7 December 2014; pp. 1–6.
10. Li, C.; Chen, Y.; Zhou, D.; Liu, J.; Zeng, J. A high-performance adaptive incremental conductance MPPT algorithm for photovoltaic systems. *Energies* **2016**, *9*, 288. [[CrossRef](#)]
11. Liu, H.D.; Lin, C.H.; Pai, K.J.; Lin, Y.L. A novel photovoltaic system control strategies for improving hill climbing algorithm efficiencies in consideration of radian and load effect. *Energy Convers. Manag.* **2018**, *165*, 815–826. [[CrossRef](#)]
12. Mohammadinodoushan, M.; Abbassi, R.; Jerbi, H.; Ahmed, F.W.; Rezvani, A. A new MPPT design using variable step size perturb and observe method for PV system under partially shaded conditions by modified shuffled frog leaping algorithm-SMC controller. *Sustain. Energy Technol. Assess.* **2021**, *45*, 101056. [[CrossRef](#)]
13. Ali, A.I.M.; Mohamed, H.R.A. Improved P&O MPPT algorithm with efficient open-circuit voltage estimation for two-stage grid-integrated PV system under realistic solar radiation. *Int. J. Electr. Power Energy Syst.* **2022**, *137*, 107805.
14. Owusu-Nyarko, I.; Elgenedy, M.A.; Abdelsalam, I.; Ahmed, K.H. Modified variable step-size incremental conductance MPPT technique for photovoltaic systems. *Electronics* **2021**, *10*, 2331. [[CrossRef](#)]
15. Yüksek, G.; Mete, A.N. A P&O Based Variable Step Size MPPT Algorithm for Photovoltaic Applications. *Gazi Univ. J. Sci.* **2023**, *36*, 608–622. [[CrossRef](#)]
16. Koad, R.B.; Zobaa, A.F.; El-Shahat, A. A novel MPPT algorithm based on particle swarm optimization for photovoltaic systems. *IEEE Trans. Sustain. Energy* **2016**, *8*, 468–476. [[CrossRef](#)]
17. Atici, K.; Sefa, I.; Altin, N. Grey wolf optimization based MPPT algorithm for solar PV system with sepic converter. In Proceedings of the 2019 4th International Conference on Power Electronics and their Applications (ICPEA), Elazig, Turkey, 25–27 September 2019; pp. 1–6.
18. González-Castaño, C.; Restrepo, C.; Kouro, S.; Rodriguez, J. MPPT algorithm based on artificial bee colony for PV system. *IEEE Access* **2021**, *9*, 43121–43133. [[CrossRef](#)]
19. Titri, S.; Larbes, C.; Toumi, K.Y.; Benatchba, K. A new MPPT controller based on the Ant colony optimization algorithm for Photovoltaic systems under partial shading conditions. *Appl. Soft Comput.* **2017**, *58*, 465–479. [[CrossRef](#)]
20. Lodhi, E.; Wang, F.Y.; Xiong, G.; Mallah, G.A.; Javed, M.Y.; Tamir, T.S.; Gao, D.W. A dragonfly optimization algorithm for extracting maximum power of grid-interfaced PV systems. *Sustainability* **2021**, *13*, 10778. [[CrossRef](#)]
21. Vankadara, S.K.; Chatterjee, S.; Balachandran, P.K.; Mihet-Popa, L. Marine predator algorithm (MPA)-based MPPT technique for solar PV systems under partial shading conditions. *Energies* **2022**, *15*, 6172. [[CrossRef](#)]
22. Mao, M.; Zhang, L.; Musembi, M.; Chong, B.; Duan, Q. Artificial fish swarm algorithm based-maximum power generation for grid-connected PV panels. In Proceedings of the 2017 UKSim-AMSS 19th International Conference on Computer Modelling & Simulation (UKSim), Cambridge, UK, 5–7 April 2017; pp. 149–154.
23. Maniraj, B.; Fathima, A.P. PV output power enhancement using whale optimization algorithm under normal and shading conditions. *Int. J. Renew. Energy Res. (IJRER)* **2020**, *10*, 1536–1543.
24. Guo, S.; Abbassi, R.; Jerbi, H.; Rezvani, A.; Suzuki, K. Efficient maximum power point tracking for a photovoltaic using hybrid shuffled frog-leaping and pattern search algorithm under changing environmental conditions. *J. Clean. Prod.* **2021**, *297*, 126573. [[CrossRef](#)]
25. Awan, M.M.A.; Asghar, A.B.; Javed, M.Y.; Conka, Z. Ordering Technique for the Maximum Power Point Tracking of an Islanded Solar Photovoltaic System. *Sustainability* **2023**, *15*, 3332. [[CrossRef](#)]
26. Awan, M.M.A.; Awan, M.J. Adapted flower pollination algorithm for a standalone solar photovoltaic system. *Mehran Univ. Res. J. Eng. Technol.* **2022**, *41*, 118–127. [[CrossRef](#)]
27. Hai, T.; Zhou, J.; Muranaka, K. An efficient fuzzy-logic based MPPT controller for grid-connected PV systems by farmland fertility optimization algorithm. *Optik* **2022**, *267*, 169636. [[CrossRef](#)]
28. Al-Majidi, S.D.; Abbod, M.F.; Al-Raweshidy, H.S. A particle swarm optimisation-trained feedforward neural network for predicting the maximum power point of a photovoltaic array. *Eng. Appl. Artif. Intell.* **2020**, *92*, 103688. [[CrossRef](#)]
29. Gaur, P. The Survey of MPPT under non-uniform atmospheric conditions for the Photovoltaic Generation Systems. *Int. J. Inf. Technol.* **2021**, *13*, 767–776.

30. Verma, D.; Nema, S.; Shandilya, A.M.; Dash, S.K. Maximum power point tracking (MPPT) techniques: Recapitulation in solar photovoltaic systems. *Renew. Sustain. Energy Rev.* **2016**, *54*, 1018–1034. [[CrossRef](#)]
31. Rasheed, M.; Alabdali, O.; Shihab, S. A New Technique for Solar Cell Parameters Estimation of The Single-Diode Model. *J. Phys. Conf. Ser.* **2021**, *1879*, 032120. [[CrossRef](#)]
32. El-sharawy, L.A.; El-helw, H.M.; Hasanien, H.M. Enhanced Grey Wolf optimization for GMPP Tracking of PV Systems under Partial Shading Condition. In Proceedings of the 2019 21st International Middle East Power Systems Conference (MEPCON), Cairo, Egypt, 17–19 December 2019; pp. 858–865.
33. Abualigah, L.; Abd Elaziz, M.; Sumari, P.; Geem, Z.W.; Gandomi, A.H. Reptile Search Algorithm (RSA): A nature-inspired meta-heuristic optimizer. *Expert Syst. Appl.* **2022**, *191*, 116158. [[CrossRef](#)]

Disclaimer/Publisher’s Note: The statements, opinions and data contained in all publications are solely those of the individual author(s) and contributor(s) and not of MDPI and/or the editor(s). MDPI and/or the editor(s) disclaim responsibility for any injury to people or property resulting from any ideas, methods, instructions or products referred to in the content.